3D MHD of Flares & Eruptions

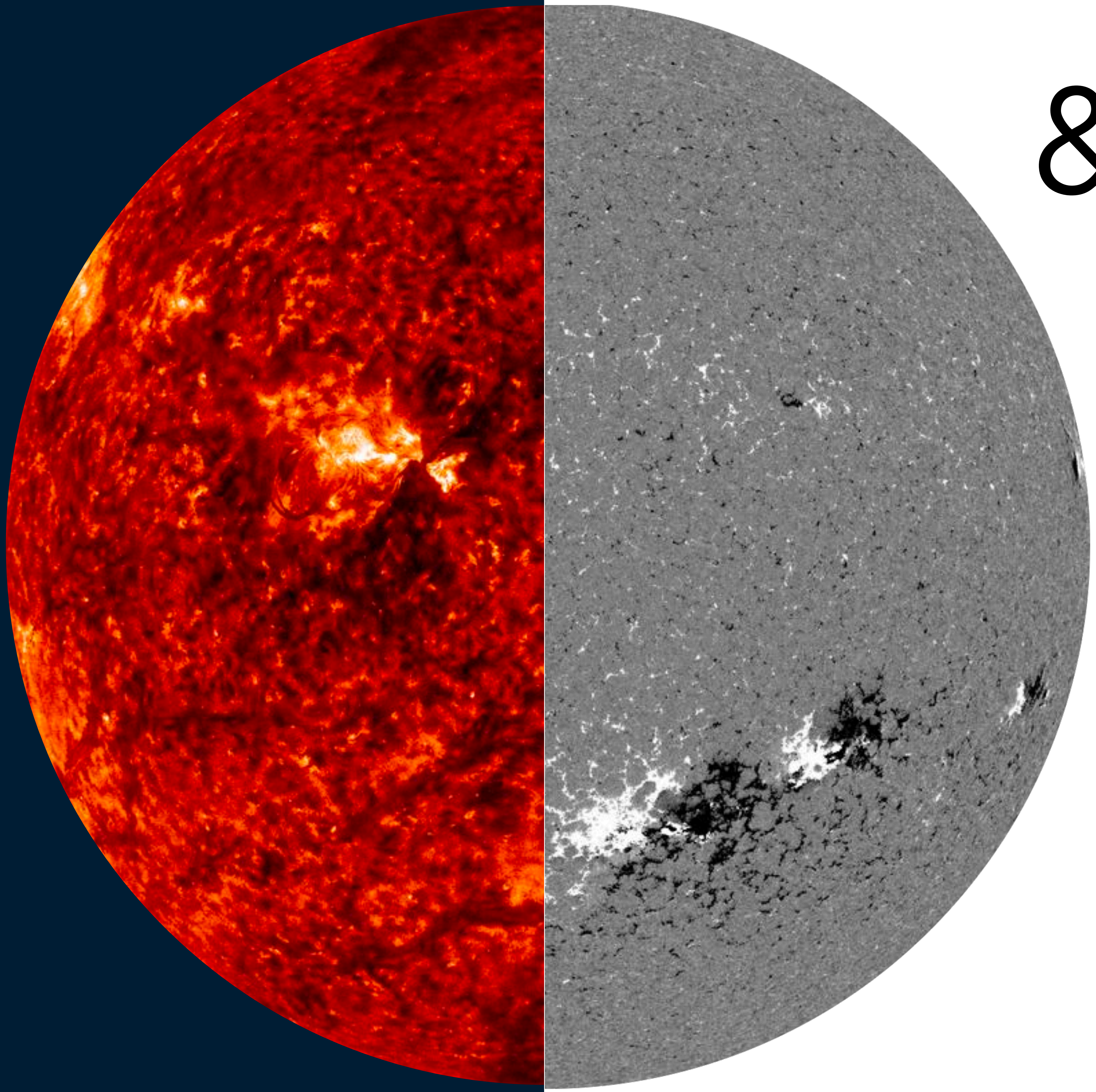

Mark Cheung, CSIRO Space & Astronomy

RoCMI 2023, Svalbard

MRO
Murchison
Geraldton
New Norcia
New Norcia
Perth
Australia Telescope Compact Array
Narrabri
Coonabarabran
Parkes
Mopra
Parkes
Sydney
Tidbinbilla
CDSCC

Inyarrimanha Ilgari Bundara*, the CSIRO Murchison Radio-astronomy Observatory

*sharing the sky and stars

Parkes Observing Schedule

Please Note: All times in this schedule are in **Australian Eastern Standard Time**.
Daylight Saving will

This is version 2 of the current schedule

April Semester 2023

Date	Day	Local Time (AEST) / Proposal	LST	Observers	Friend	Receiver
01 Apr	Sat	00:00 - 12:00 **Director's Time**	12:27 - 00:29	.	.	.
		12:00 - 13:00 **P1189** A pulsar-based solar space weather monitoring network(Zic)	00:29 - 01:29	Zic...	ops-team	UWL
		13:00 - 24:00 **P456** A millisecond pulsar timing array(Hobbs)	01:29 - 12:31	Hobbs...	ops-team	UWL
02 Apr	Sun	00:00 - 12:00 **P456** A millisecond pulsar timing array(Hobbs)	12:31 - 00:33	Hobbs...	ops-team	UWL
		12:00 - 13:00 **P1189** A pulsar-based solar space weather monitoring network(Zic)	00:33 - 01:33	Zic...	ops-team	UWL
		13:00 - 21:00 **P456** A millisecond pulsar timing array(Hobbs)	01:33 - 09:35	Hobbs...	ops-team	UWL
		21:00 - 24:00 **Director's Time**	09:35 - 12:35	.	.	.
03 Apr	Mon	00:00 - 02:00 **P1050** Initial Follow-up of New Pulsar Discoveries from Re-processing of the HTRU-S LowLat Galactic Plane Survey(Sengar)	12:35 - 14:36	Sengar...	ops-team	UWL
		02:00 - 03:00 **P885** Understanding the Remarkable Behaviour of Radio Magnetars(Camilo)	14:36 - 15:36	Camilo...	ops-team	UWL
		03:00 - 05:00 **P1101** Monitoring FRB190520 with the Parkes Ultra-Wideband Low receiver(Dai)	15:36 - 17:36	Dai...	ops-team	UWL
		05:00 - 08:30 **P1192** Timing the First Seven Pulsars Discovered in Terzan 1(DeCesar)	17:36 - 21:07	DeCesar...	ops-team	UWL
		08:30 - 10:00 **Director's Time**	21:07 - 22:37	.	.	.
		10:00 - 11:00 **P1189** A pulsar-based solar space weather monitoring network(Zic)	22:37 - 23:37	Zic...	ops-team	UWL
		11:00 - 13:30 **P1183** Studying the radiation spectrum and polarization of a new energetic FRB 20220529(Zhang)	23:37 - 02:07	Zhang...	ops-team	UWL
		13:30 - 24:00 **P574** Young Pulsar Timing: Probing the Physics of Pulsars and Neutron Stars(Lower)	02:07 - 12:39	Lower...	ops-team	UWL
04 Apr	Tue	00:00 - 10:30 **P574** Young Pulsar Timing: Probing the Physics of Pulsars and Neutron Stars(Lower)	12:39 - 23:11	Lower...	ops-team	UWL
		10:30 - 12:30 **P595** PULSE@Parkes (Pulsar Student Exploration online at Parkes)(Hobbs)	23:11 - 01:11	Hobbs...	ops-team	UWL
		12:30 - 13:30 **P1189** A pulsar-based solar space weather monitoring network(Zic)	01:11 - 02:11	Zic...	ops-team	UWL
		13:30 - 14:30 **Director's Time**	02:11 - 03:12	.	.	.
		14:30 - 18:00 **P455** Timing and geodetic precession in the double pulsar(Burgay)	03:12 - 06:42	Burgay...	ops-team	UWL
		18:00 - 20:00 **P1054** Follow-up of pulsar discoveries from MeerKAT searches(Burgay)	06:42 - 08:42	Burgay...	ops-team	UWL
		20:00 - 24:00 **P1032** Timing southern binary pulsar systems(Venkatraman Krishnan)	08:42 - 12:43	Venkatraman Krishnan...	ops-team	UWL
05 Apr	Wed	00:00 - 02:00 **P1032** Timing southern binary pulsar systems(Venkatraman Krishnan)	12:43 - 14:43	Venkatraman Krishnan...	ops-team	UWL
		02:00 - 04:00 **P1054** Follow-up of pulsar discoveries from MeerKAT searches(Burgay)	14:43 - 16:44	Burgay...	ops-team	UWL
		04:00 - 06:00 **P1194** Identifying millisecond pulsars among the candidates selected from Fermi LAT(Lu)	16:44 - 18:44	Lu...	ops-team	UWL
		06:00 - 08:00 **P1054** Follow-up of pulsar discoveries from MeerKAT searches(Burgay)	18:44 - 20:44	Burgay...	ops-team	UWL
		08:00 - 16:00 **Maintenance**	20:44 - 04:46	.	.	.
		16:00 - 24:00 **PX500** FAST: category 1 purchased time(Li)	04:46 - 12:47	Li...	ops-team	UWL

"What is the state of the art of 3D MHD simulations of flares and eruptions, and how do synthetic observables compare with observations?

Which physical mechanisms are missing and which modelling advances are needed, also given the future availability of high-resolution observations from MUSE and other missions?"

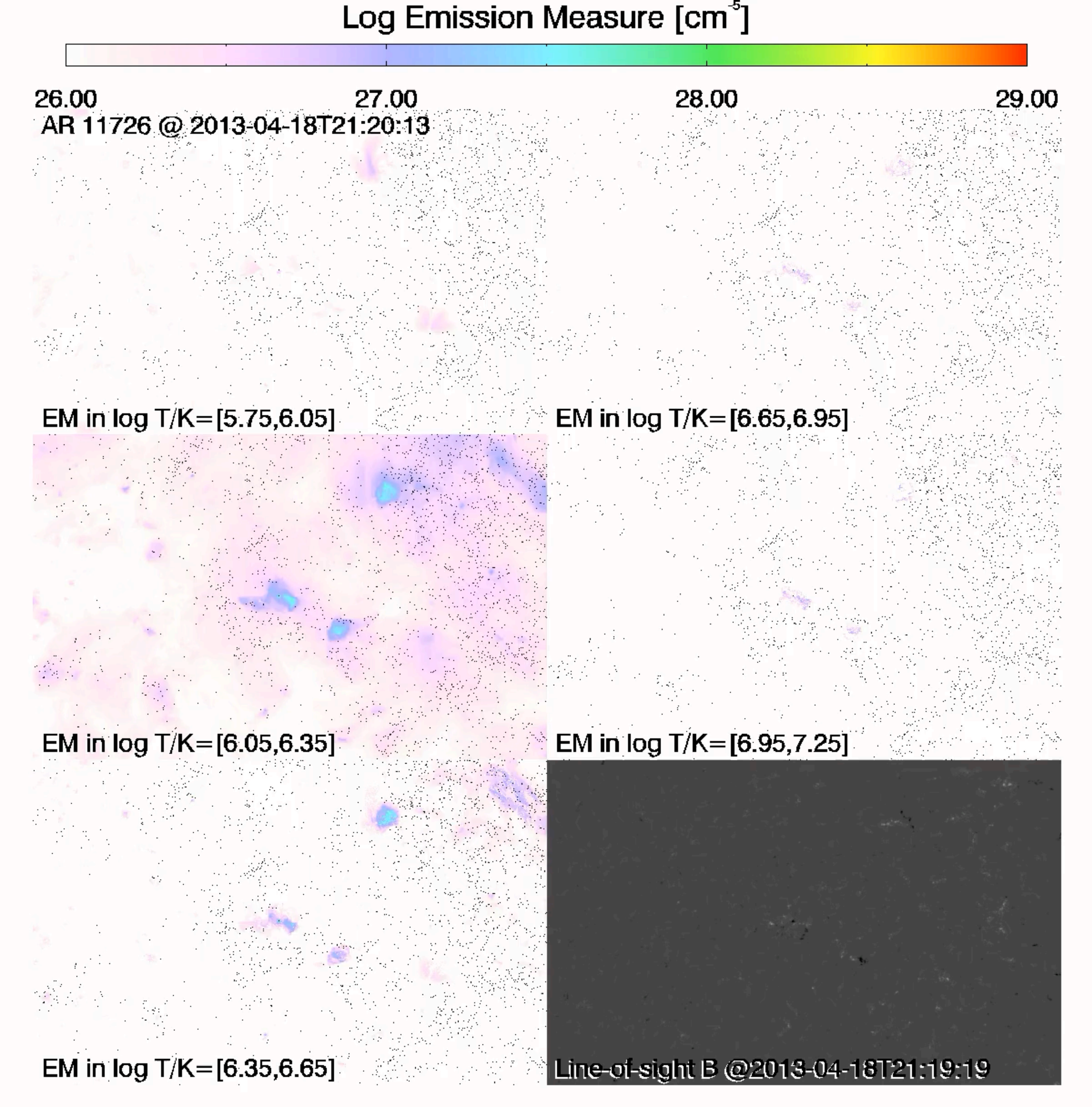

[DEM movie of the emergence of AR 11726]()

Other panels:
EM in various log T bins

Lower right panel only
Greyscale:
B_{los} from HMI
Yellow/Green: 6MK EM
Red: 10 MK EM

DEM movie
of the emergence
of AR 11726

Greyscale:
B_{los} from HMI
Green: 6MK EM
Yellow/Red: 10 MK EM

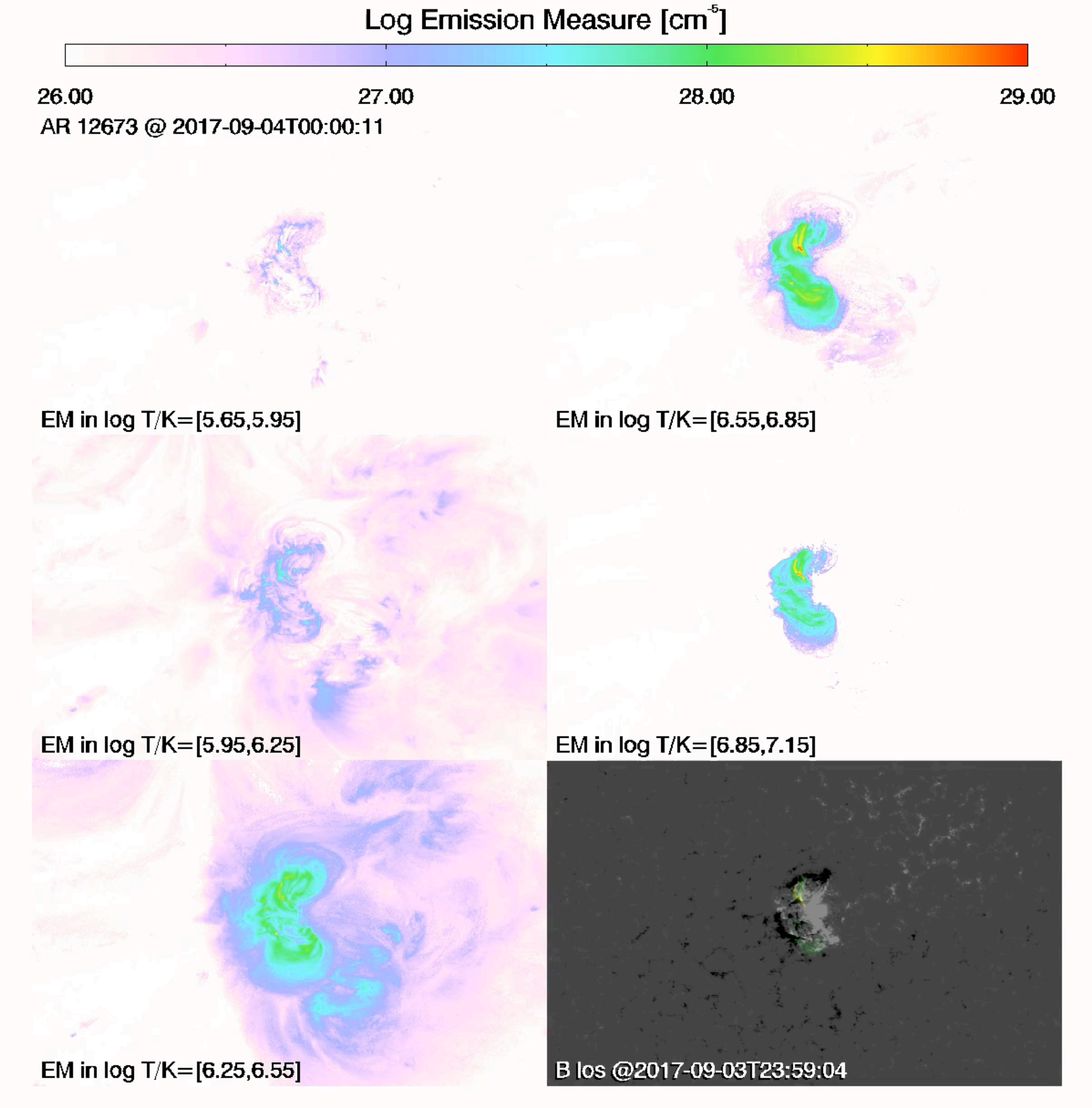

DEM movie of the emergence of AR 12673

Other panels:
EM in various log T bins

Lower right panel only
Greyscale:
B_{los} from HMI
Yellow/Green: 6MK EM
Red: 10 MK EM

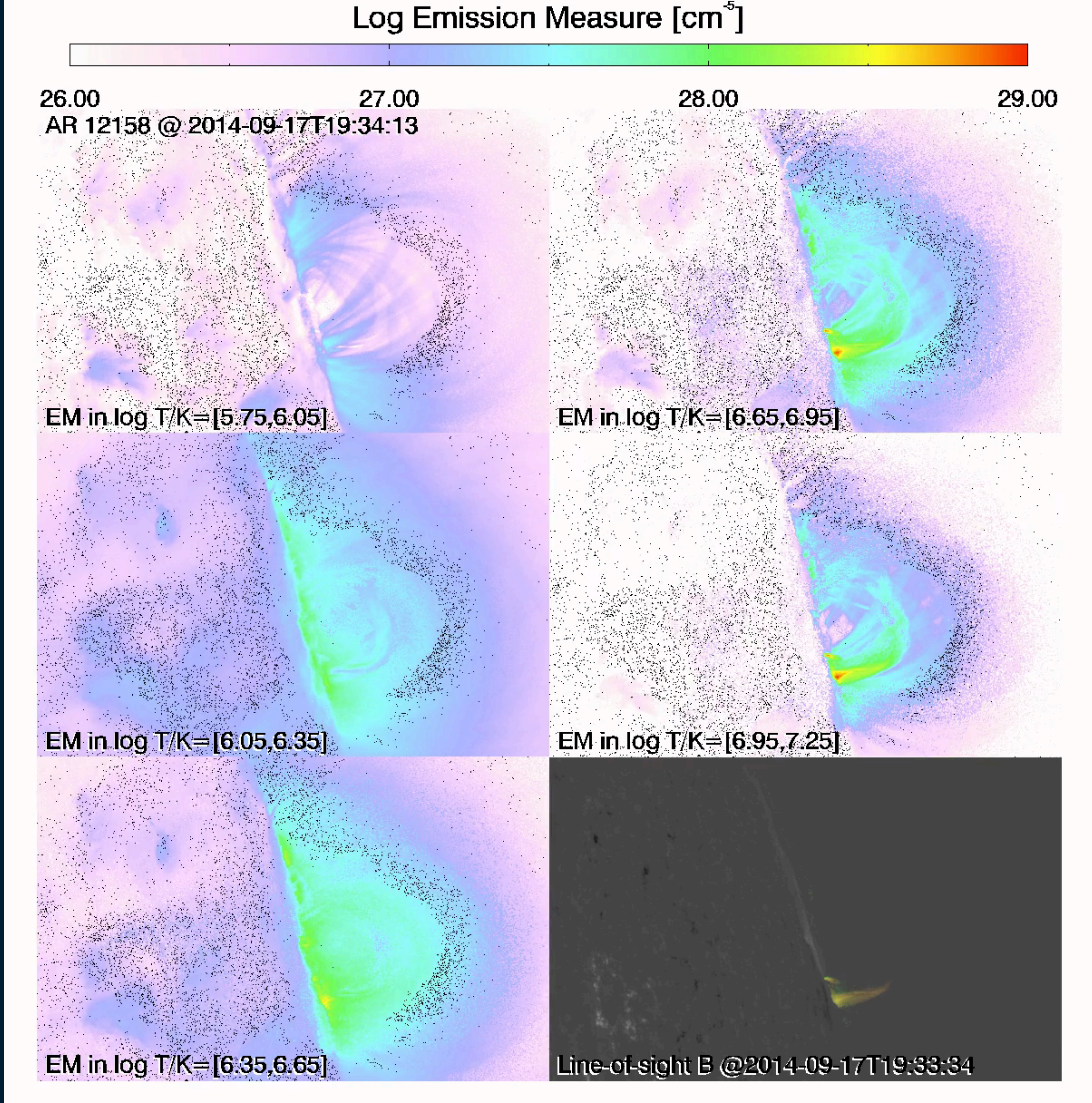

Other panels:
EM in various log T bins

- **Tell-tale signs of chromospheric evaporation**
- **Loops filled with plasma at 10 MK and above**
- **Loops cool to lower log T bins**
- **At time (~20:29 UT) when plasma cools down to log T/K ~ 5.8, coronal condensations in SJI 1330 begin to appear.**

Lower right panel only
Greyscale:
B_{los} from HMI
Yellow/Green: 6MK EM
Red: 10 MK EM

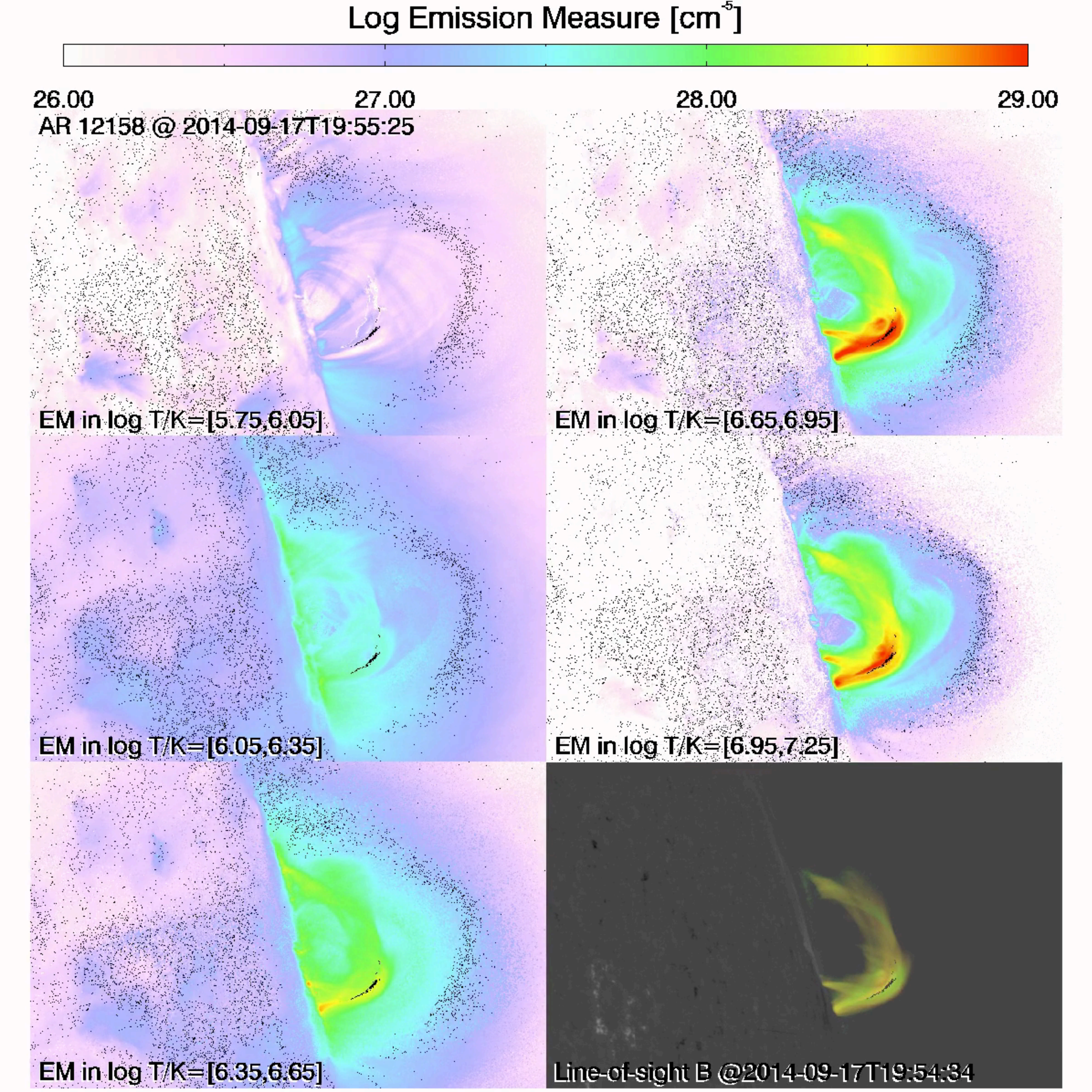

Other panels:
EM in various log T bins

- **Tell-tale signs of chromospheric evaporation**
- **Loops filled with plasma at 10 MK and above**
- **Loops cool to lower log T bins**
- **At time (~20:29 UT) when plasma cools down to log T/K ~ 5.8, coronal condensations in SJI 1330 begin to appear.**

Lower right panel only
Greyscale:
B_{los} from HMI
Yellow/Green: 6MK EM
Red: 10 MK EM

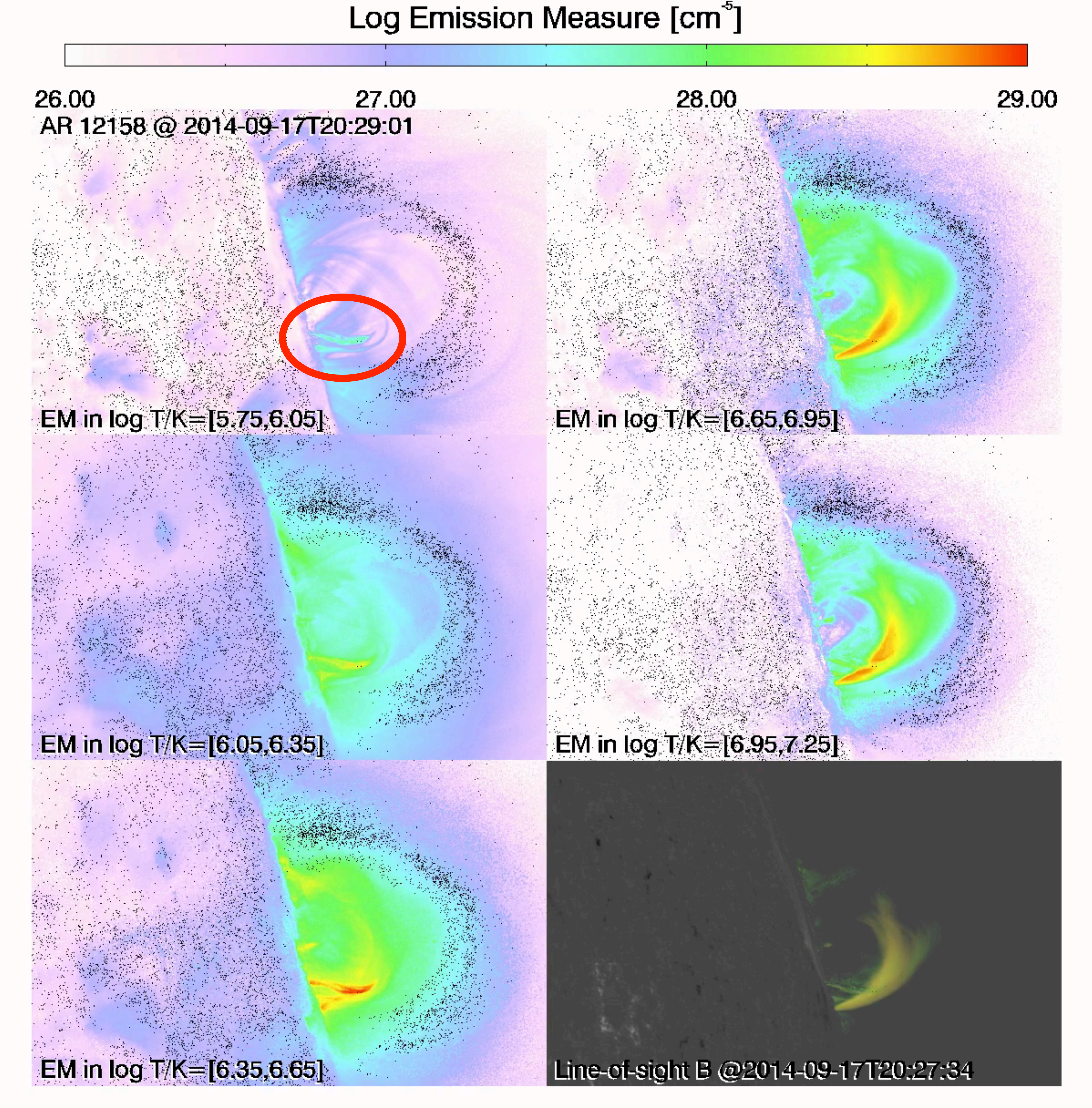

Other panels:
EM in various log T bins

- **Tell-tale signs of chromospheric evaporation**
- **Loops filled with plasma at 10 MK and above**
- **Loops cool to lower log T bins**
- **At time (~20:29 UT) when plasma cools down to log T/K ~ 5.8, coronal condensations in SJI 1330 begin to appear.**

Lower right panel only
Greyscale:
B_{los} from HMI
Yellow/Green: 6MK EM
Red: 10 MK EM

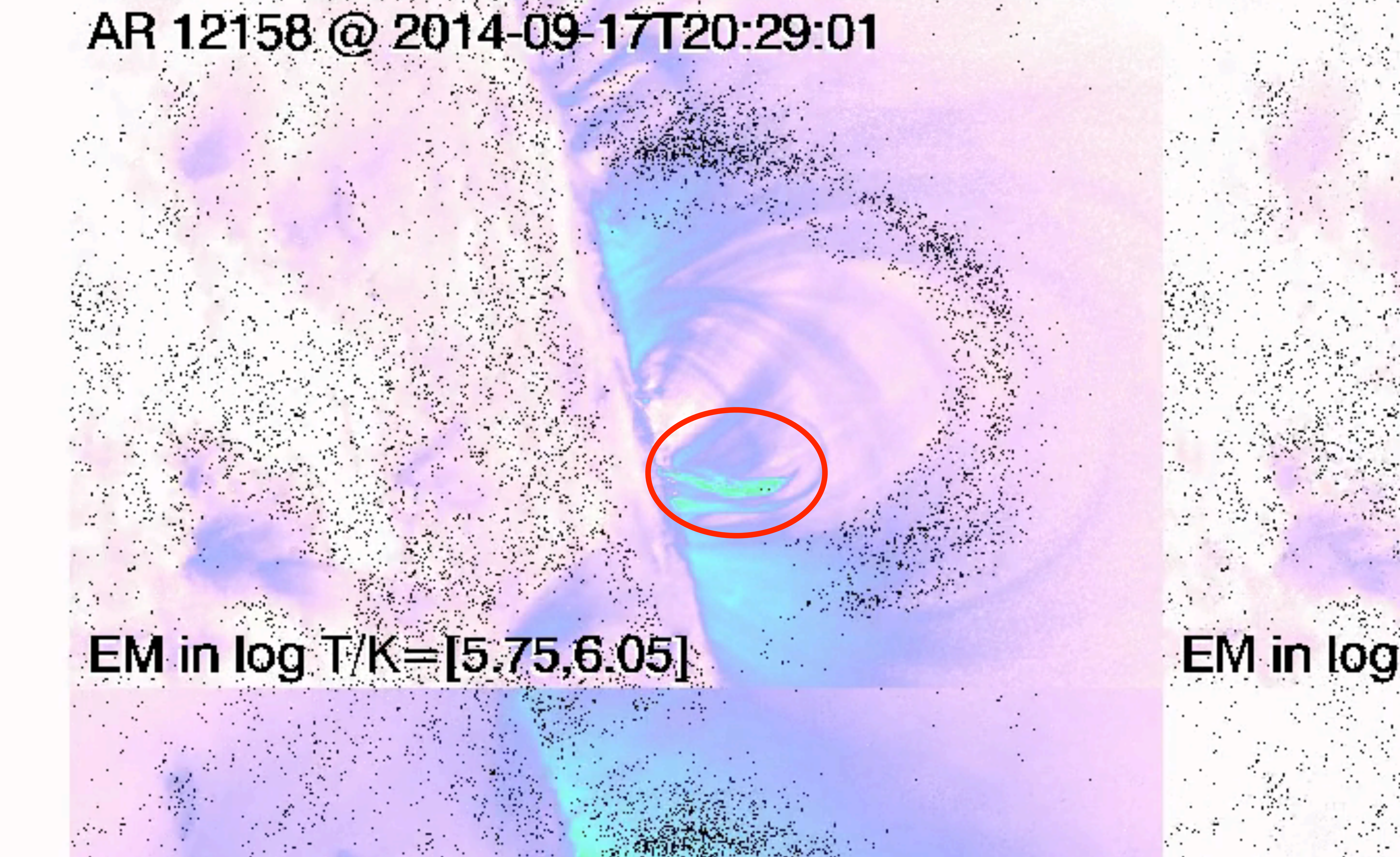

AR 12158 @ 2014-09-17T20:29:01
EM in log T/K=[5.75,6.05]
EM in log

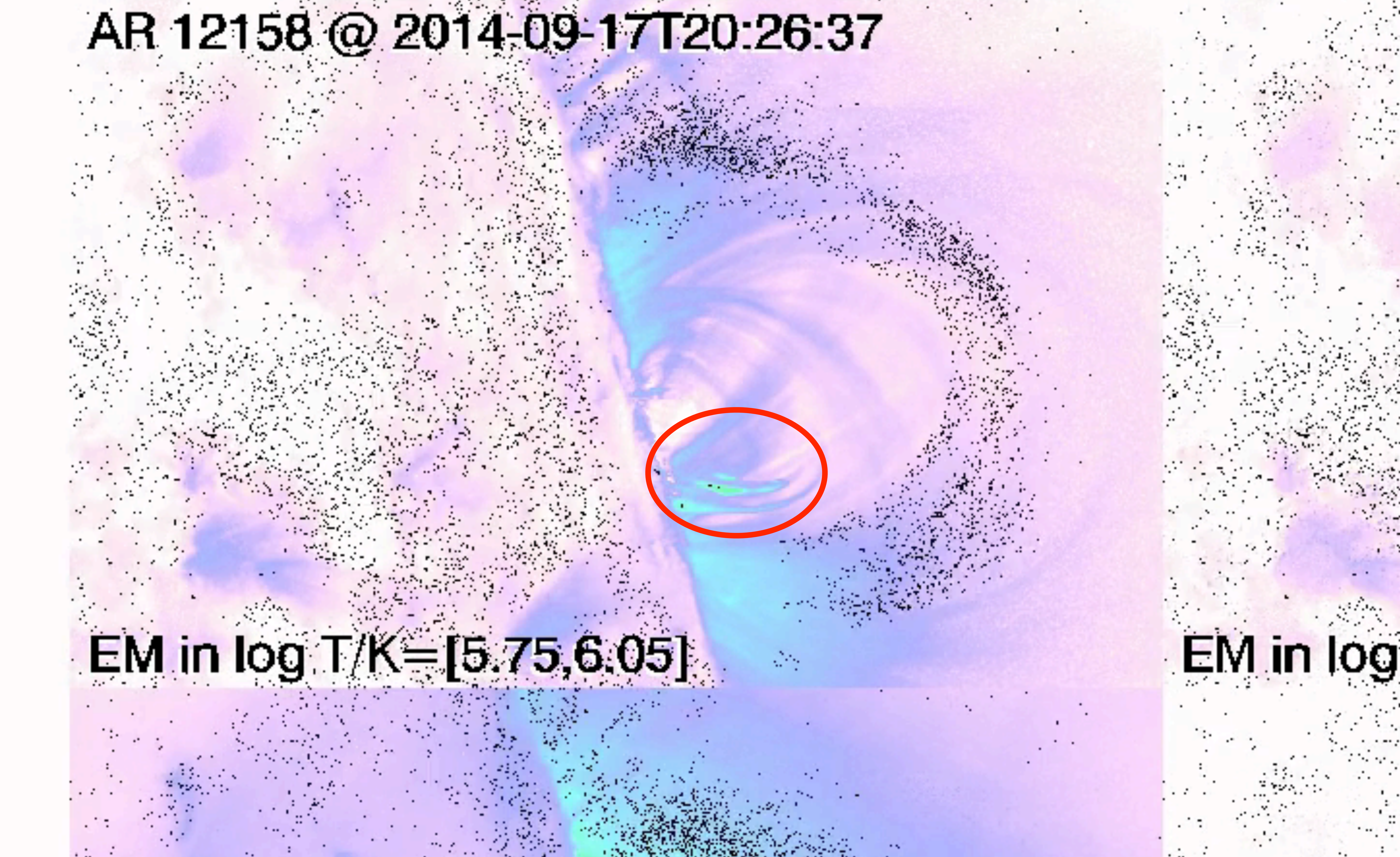
AR 12158 @ 2014-09-17T20:26:37
EM in log T/K=[5.75,6.05]
EM in log

IRIS SJI 1330: Coronal condensations appear at about same time (~20:29 UT) as when AIA sees sub-MK plasma.

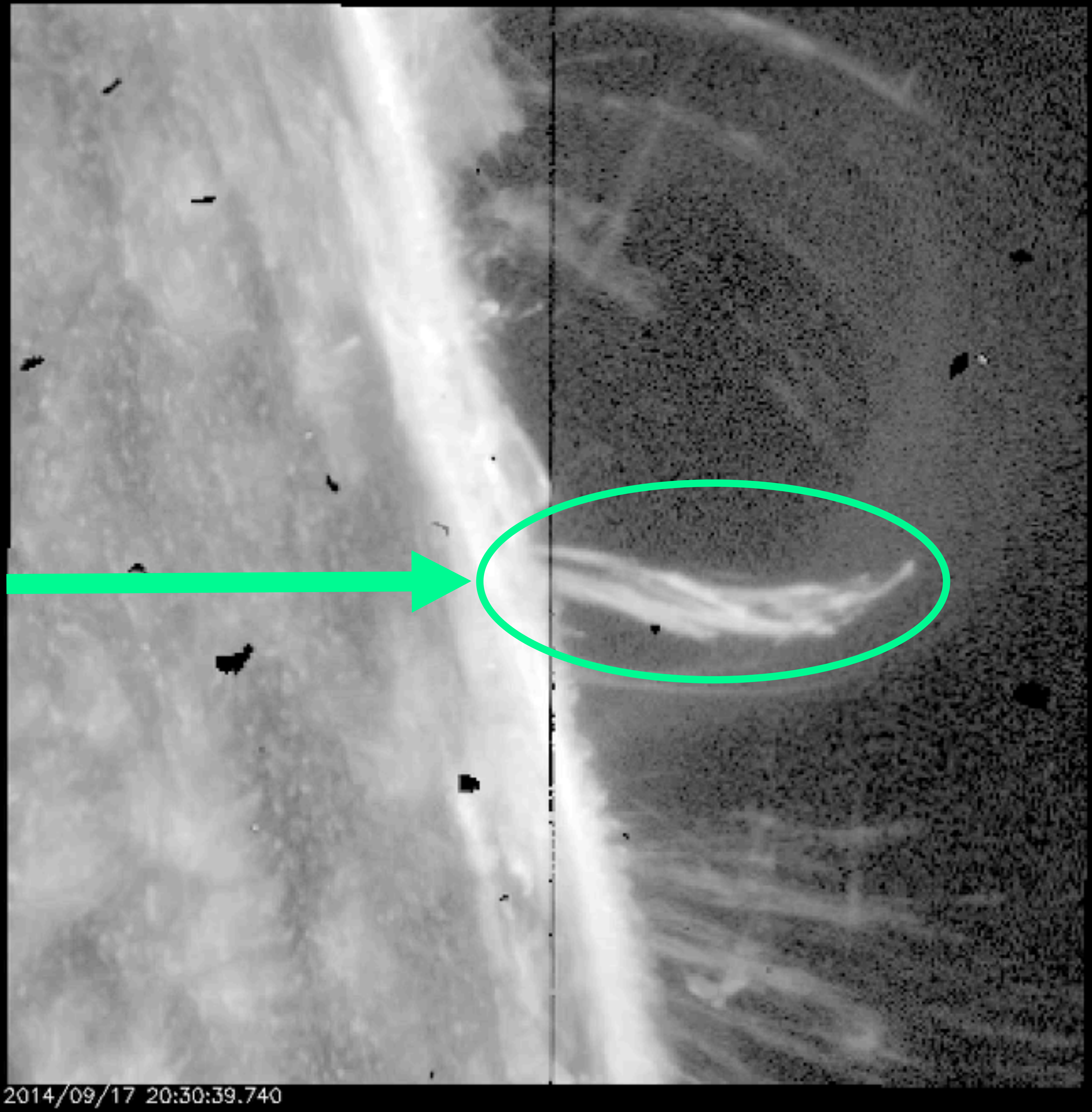

Are there nanojets?

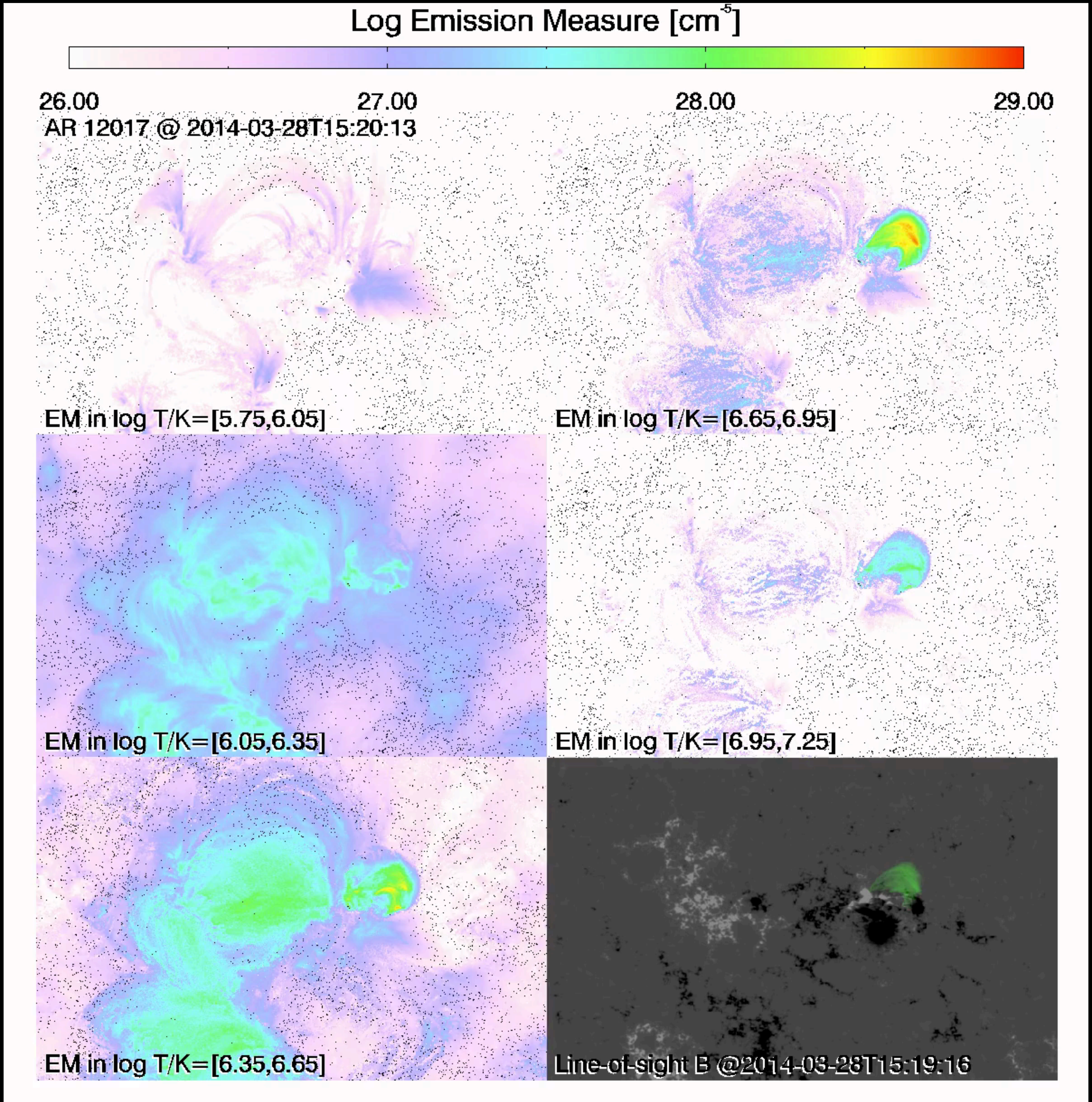

<u>NOAA AR 12017:</u>
one X-class ("Best Observed X-flare"), 3 M-class, and about two dozen C-class flares

Sunquake: Judge et al. (2014)
Filament Eruption before X-flare: Kleint et al. (2015)
IRIS Fe XXI FUV spectra: Young et al. (2015)
Chromospheric Evaporation: Li et al. (2015)

A comprehensive three-dimensional radiative magnetohydrodynamic simulation of a solar flare

published November 26th 2018 in Nature Astronomy
https://doi.org/10.1038/s41550-018-0629-3

M. C. M. Cheung, M. Rempel, G. Chintzoglou, F. Chen, P. Testa, J. Martínez-Sykora, A. Sainz Dalda, M. L. DeRosa, A. Malanushenko, V. Hansteen, B. De Pontieu, M. Carlsson, B. Gudiksen & S. W. McIntosh

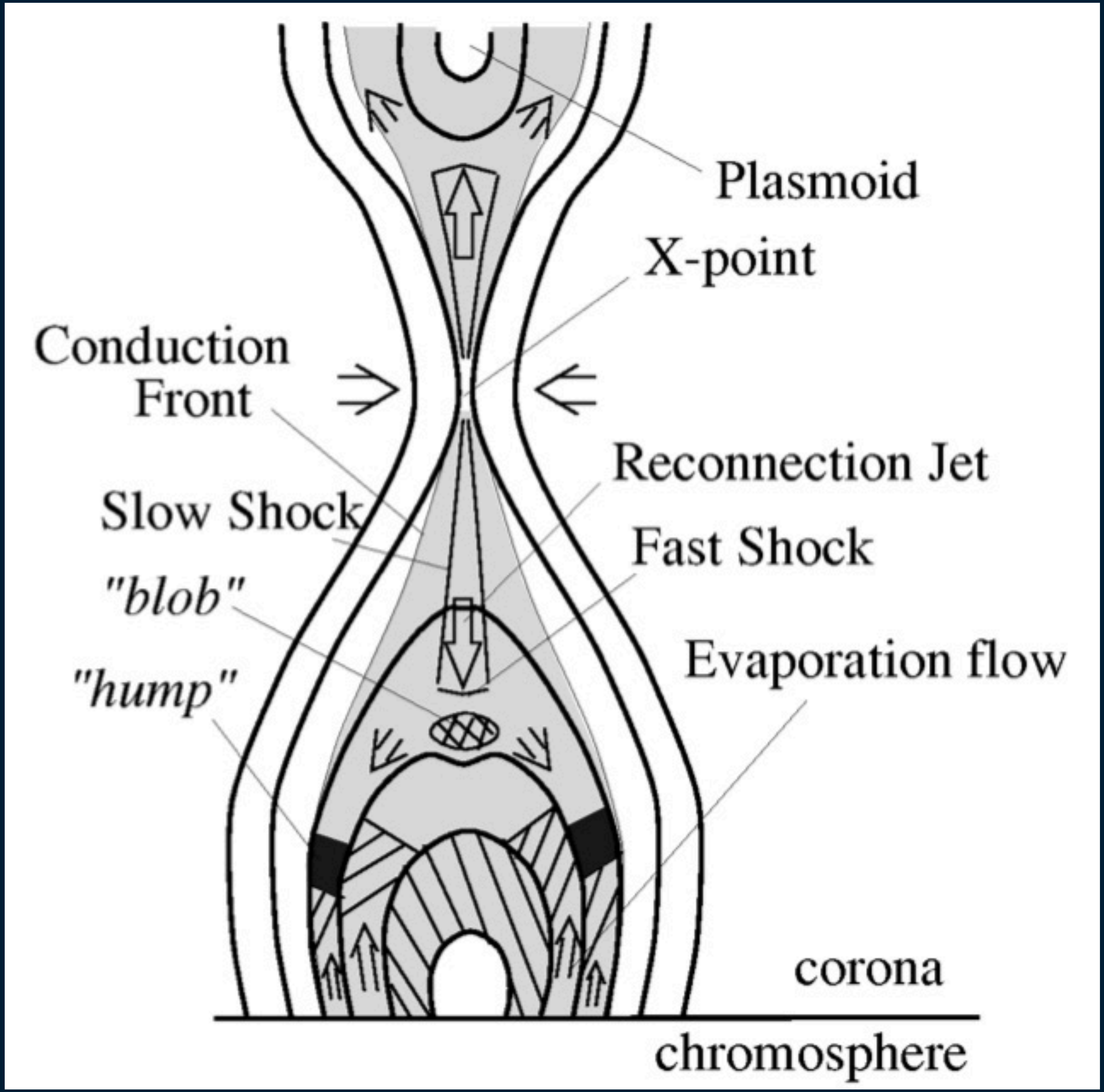

Yokoyama & Shibata (1998)

- 2D MHD model of flare reconnection.

- The efficient transport of energy released by reconnection is modeled as thermal conduction carried by electrons streaming along field lines.

- Energy dumped into the chromosphere leads to dense upflows (humps): "chromospheric evaporation"

- The model predicts density enhancement in the termination region ("blob").

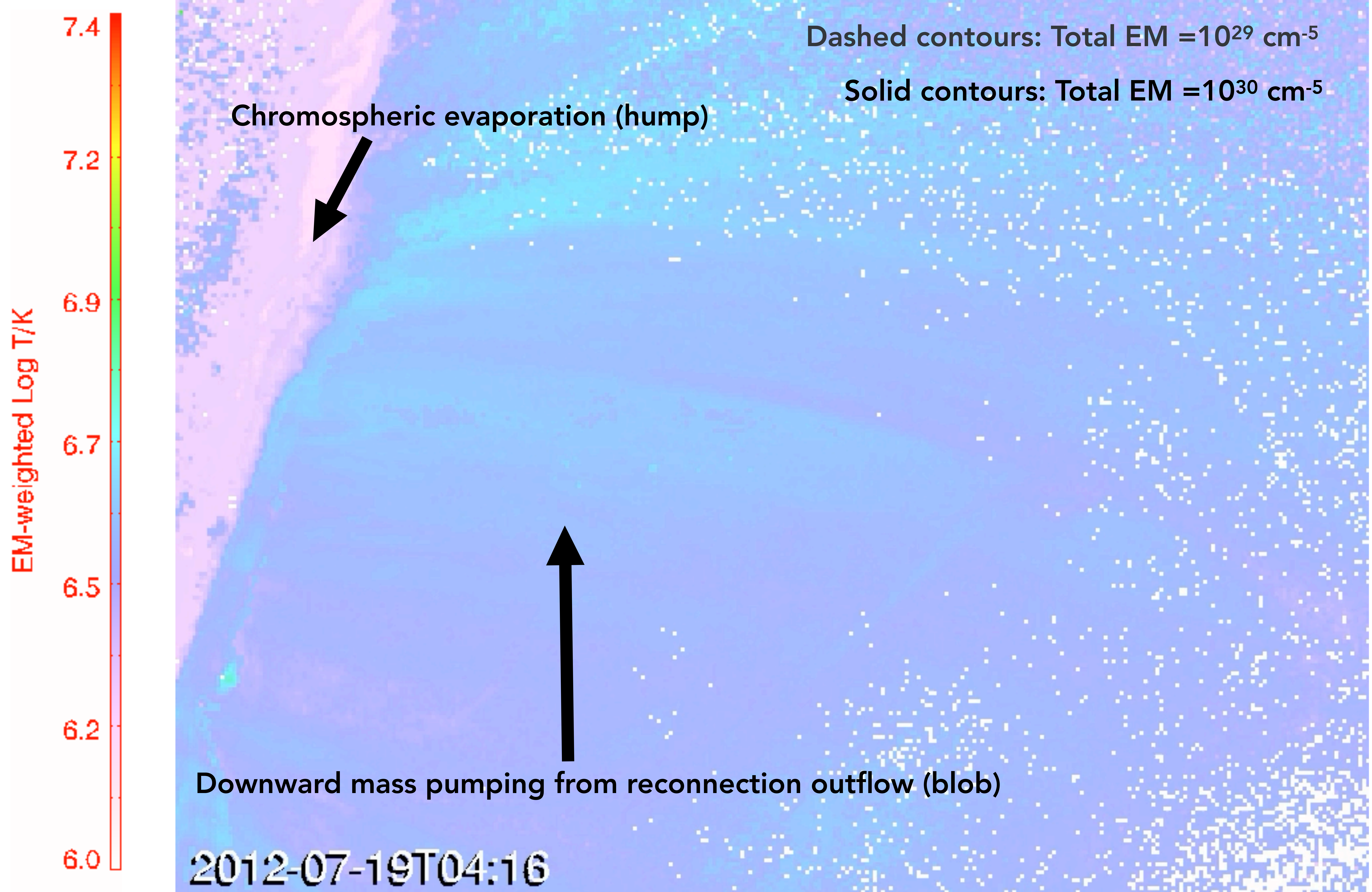
Dashed contours: Total EM =10^29 cm^-5
Solid contours: Total EM =10^30 cm^-5
Chromospheric evaporation (hump)
Downward mass pumping from reconnection outflow (blob)
2012-07-19T04:16
EM-weighted Log T/K
7.4
7.2
6.9
6.7
6.5
6.2
6.0

Figure 1. Number density *Ne* (in cm–3), temperature *Te* (in MK), and vertical velocity *vy* (in 100 km s–1) at *t* = 40, 80, and 120 s. In the temperature views (middle row), white and yellow contours near the flare loop footpoints show the heating due to fast electron energy deposition, with a level of 1% and 10% of the maximum values, respectively. In the same panels, the black contour identifies the instantaneous region of fast electron energization.

Ruan, Xia & Keppens (2020)

Synthetic GOES X-ray Light Curves

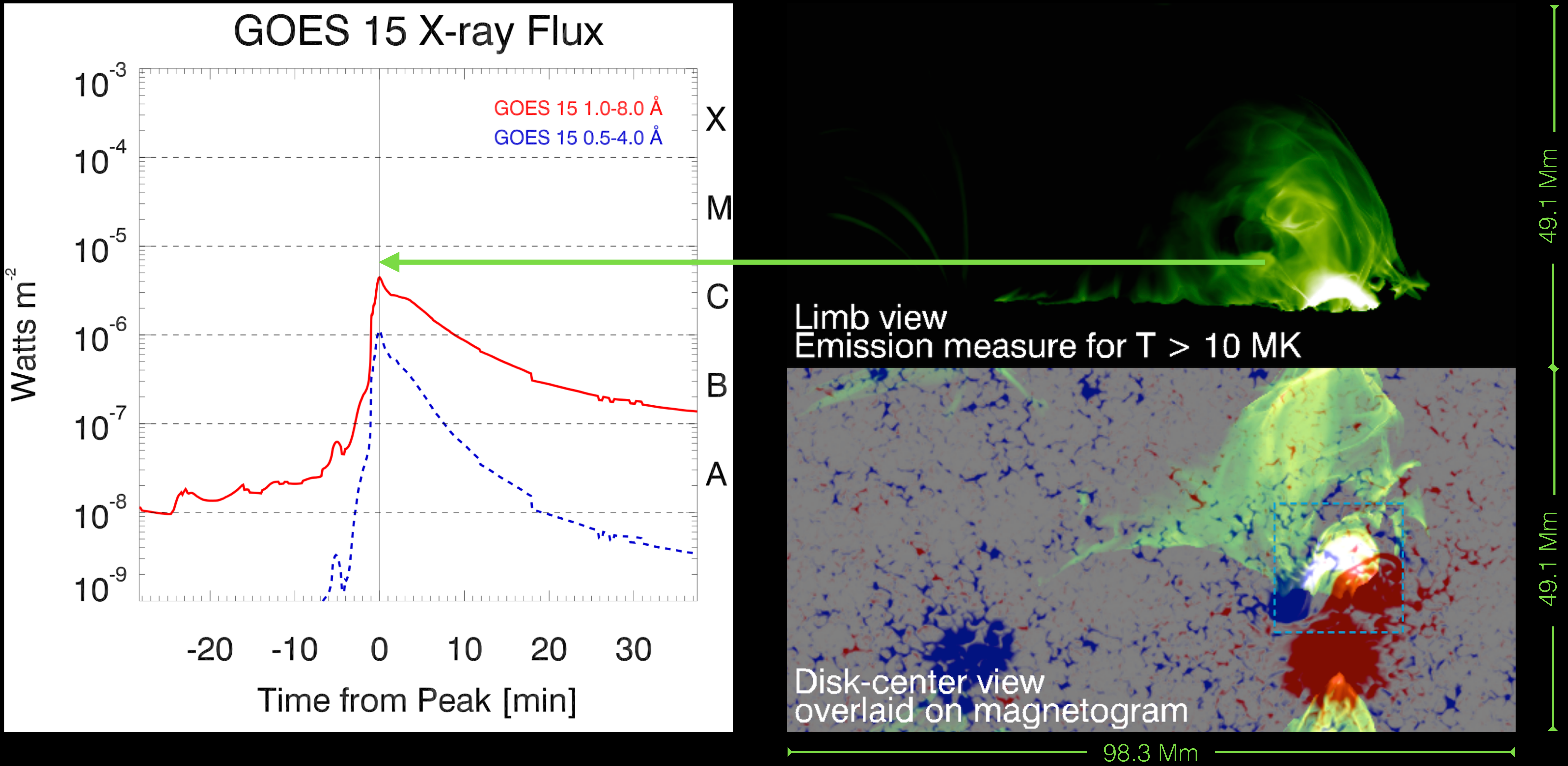

C4 flare if measured by detectors on GOES 15. The free magnetic energy (actual minus potential field) dropped by ~5x10^{30} erg (~10%) over 5 minutes.

Synthetic Doppler Maps: scaled by DEM

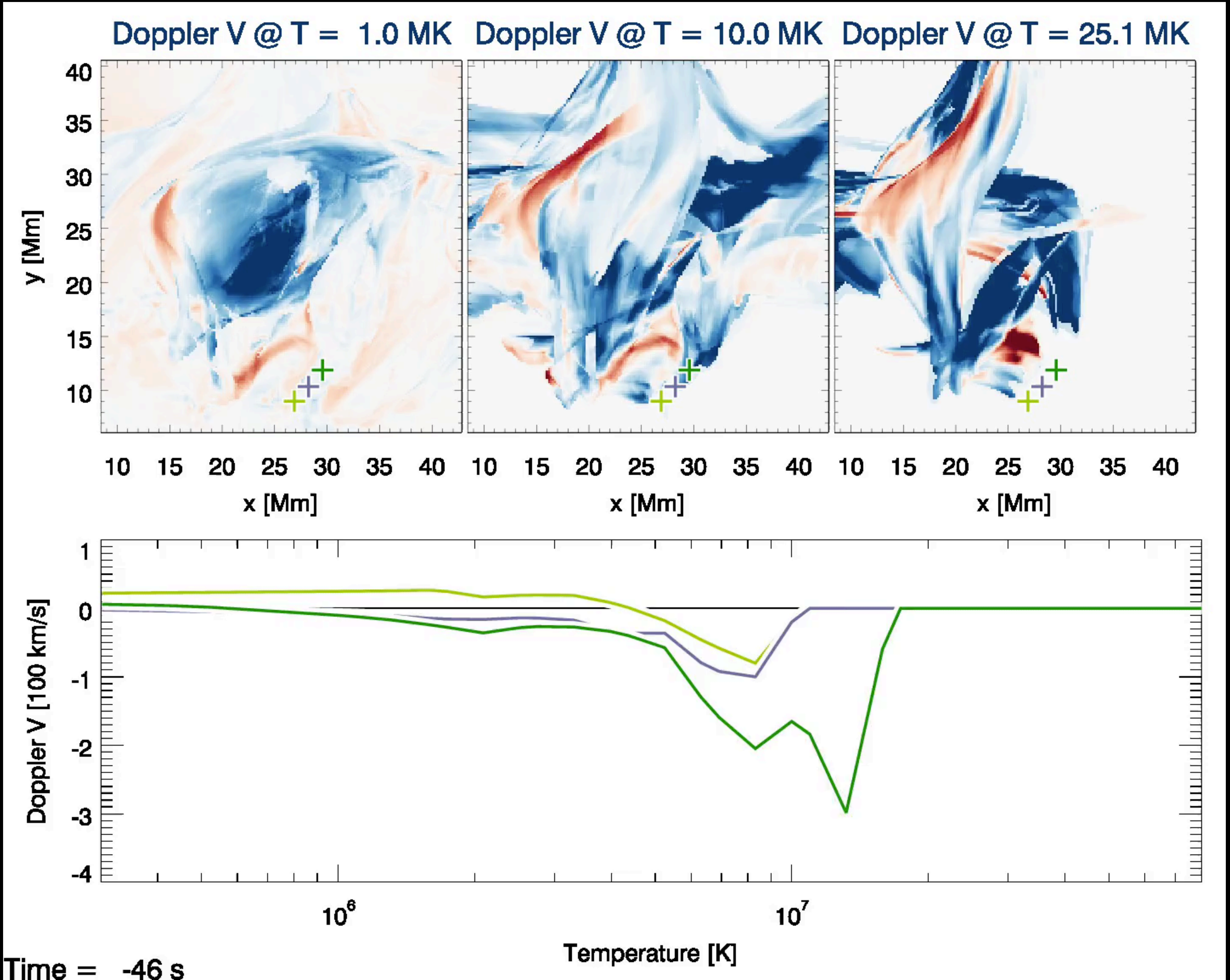

Using only thermal bremsstrahlung (+lines), the model yields power law-like shapes for the X-ray spectrum.

The multi-thermal nature of the magnetic structure gives rise to the apparent non-thermal behavior.

Above-the-loop-top harder X-ray sources (> 25 keV) are located above softer loop sources.

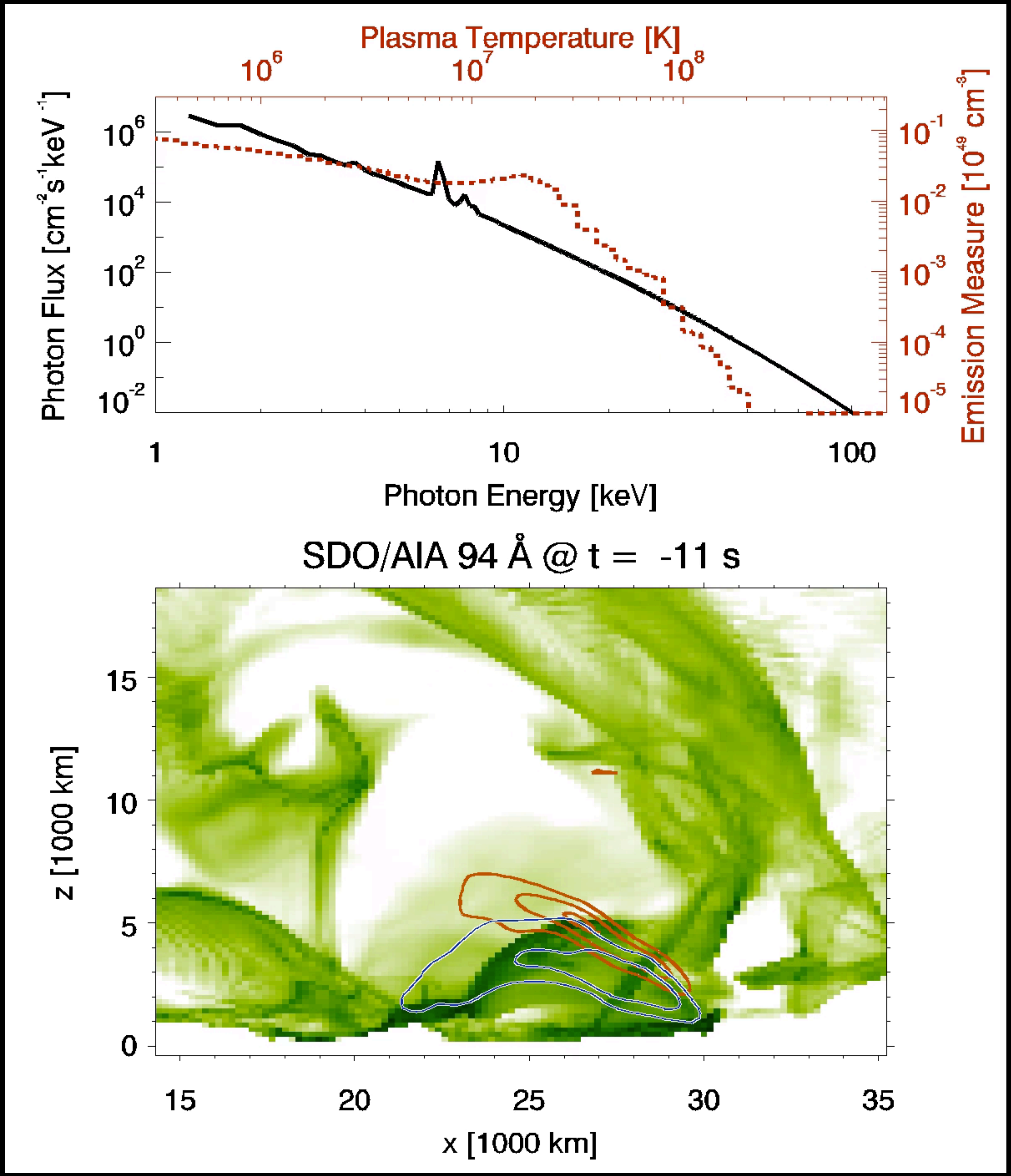

Hard x-rays ≥ 25 keV 6 ≤ Soft x-rays ≤ 12 keV

Xiaocan Li *et al* 2017 *ApJ* **843** 21: 2D PIC simulations (Maxwell + relativistic Vlasov equations) of particle acceleration (mass ratios m_p/m_e up to 100)

- Robust w.r.t. mass ratio: "reconnection rate, magnetic energy conversion, ion internal energy gain, plasma energization processes, ion energy spectra"

- Sensitive to mass ratio: "electrons gain more energy (internal or kinetic) in runs with lower mass ratios"

- "the accelerated electron distribution is actually a superposition of a series of different distributions, <u>but each distribution only has a small non-thermal component relative to its thermal component.</u> "

Xiaocan Li *et al* 2019 *ApJ* **879** 5: extended to mass ratio = 400

Xiaocan Li *et al* 2017 *ApJ* **843** 21

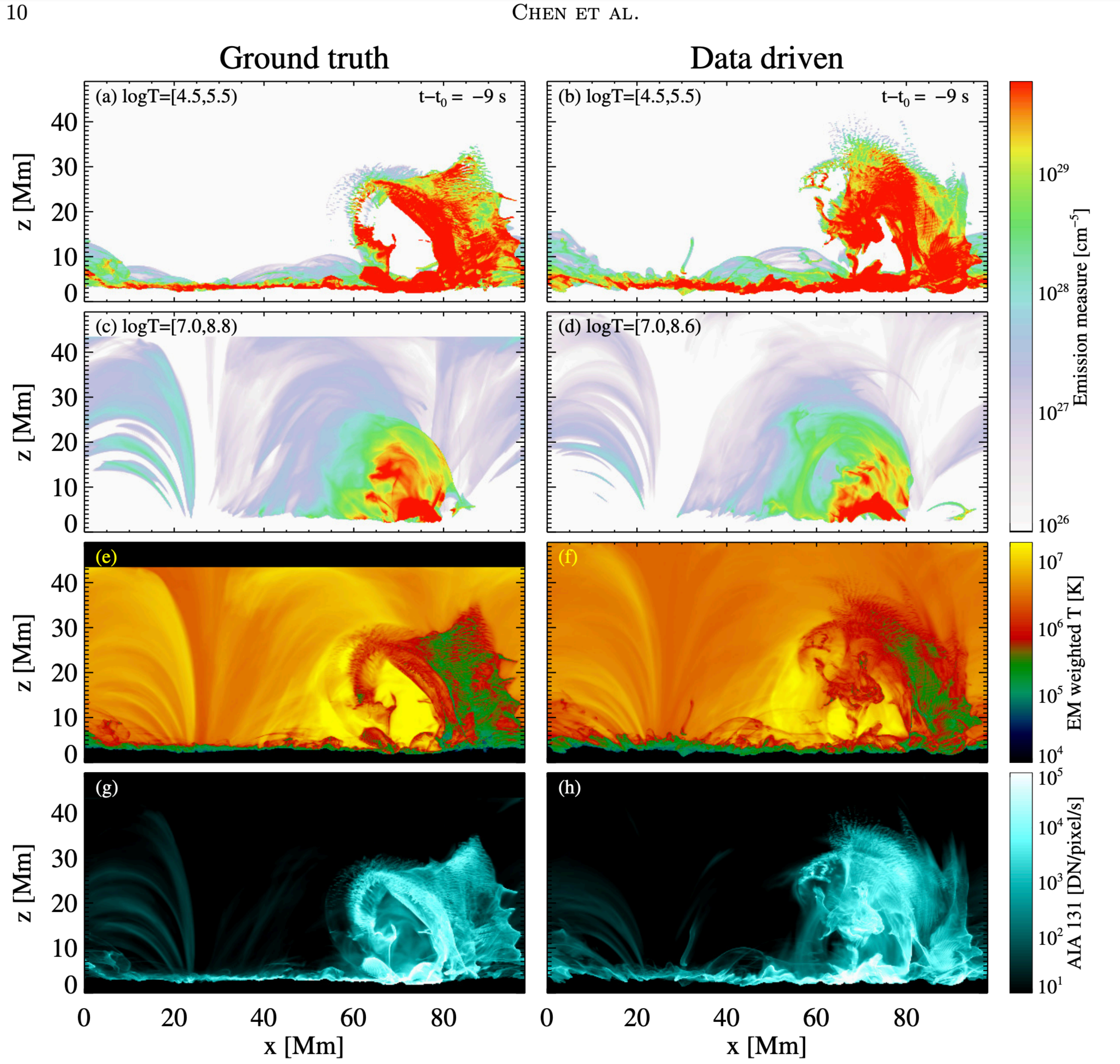

Chen et al. (under review)

- MURaM-data-driven, MURaM simulation of a flare.
- Sampled electric fields at the photosphere to drive an initial potential field distribution.
- Quantitative differences between different numerical setups (e.g. grid spacing).

The Astrophysical Journal, 926:53 (32pp), 2022 February 10 https://doi.org/10.3847/1538-4357/ac4223

Probing the Physics of the Solar Atmosphere with the Multi-slit Solar Explorer (MUSE). II. Flares and Eruptions

Mark C. M. Cheung[1], Juan Martínez-Sykora[1,2,3,4], Paola Testa[5], Bart De Pontieu[1,3,4], Georgios Chintzoglou[1,6], Matthias Rempel[7], Vanessa Polito[1,2], Graham S. Kerr[8,9], Katharine K. Reeves[5], Lyndsay Fletcher[3,10], Meng Jin[1,11], Daniel Nóbrega-Siverio[3,4,12,13], Sanja Danilovic[14], Patrick Antolin[15], Joel Allred[9], Viggo Hansteen[1,2,3,4], Ignacio Ugarte-Urra[16], Edward DeLuca[5], Dana Longcope[17], Shinsuke Takasao[18], Marc L. DeRosa[1], Paul Boerner[1], Sarah Jaeggli[19], Nariaki V. Nitta[1], Adrian Daw[9], Mats Carlsson[3,4], and Leon Golub[5]
The *MUSE* team

[1] Lockheed Martin Solar & Astrophysics Laboratory, 3251 Hanover St, Palo Alto, CA 94304, USA; cheung@lmsal.com
[2] Bay Area Environmental Research Institute, NASA Research Park, Moffett Field, CA 94035, USA
[3] Rosseland Centre for Solar Physics, University of Oslo, P.O. Box 1029 Blindern, NO-0315 Oslo, Norway
[4] Institute of Theoretical Astrophysics, University of Oslo, P.O. Box 1029 Blindern, NO-0315 Oslo, Norway
[5] Harvard-Smithsonian Center for Astrophysics, 60 Garden St, Cambridge, MA 02193, USA
[6] University Corporation for Atmospheric Research, Boulder, CO 80307-3000, USA
[7] High Altitude Observatory, NCAR, P.O. Box 3000, Boulder, CO 80307, USA
[8] Department of Physics, The Catholic University of America, 620 Michigan Avenue NW, Washington DC 20064, USA
[9] NASA Goddard Space Flight Center, Heliophysics Sciences Division, Code 671, 8800 Greenbelt Road, Greenbelt, MD 20771, USA
[10] SUPA School of Physics & Astronomy, University of Glasgow, Glasgow, G12 8QQ, UK
[11] SETI Institute, 189 North Bernardo Avenue, Suite 200, Mountain View, CA 94043, USA
[12] Instituto de Astrofísica de Canarias, E-38205 La Laguna, Tenerife, Spain
[13] Universidad de La Laguna, Dept. Astrofísica, E-38206 La Laguna, Tenerife, Spain
[14] Institute for Solar Physics, Department of Astronomy, Stockholm University, AlbaNova University Centre, SE-106 91 Stockholm, Sweden
[15] Department of Mathematics, Physics & Electrical Engineering, Northumbria University, Newcastle Upon Tyne, NE1 8ST, UK
[16] Space Science Division, Naval Research Laboratory, Washington, DC 20375, USA
[17] Department of Physics, Montana State University, Bozeman, MT 59717, USA
[18] Department of Earth and Space Science, Graduate School of Science, Osaka University, Toyonaka, Osaka 560-0043, Japan
[19] National Solar Observatory, 22 Ohi'a Ku, Makawao, HI 96768, USA
Received 2021 August 20; revised 2021 December 6; accepted 2021 December 9; published 2022 February 11

MUSE will constrain initiation mechanisms of flares and CMEs

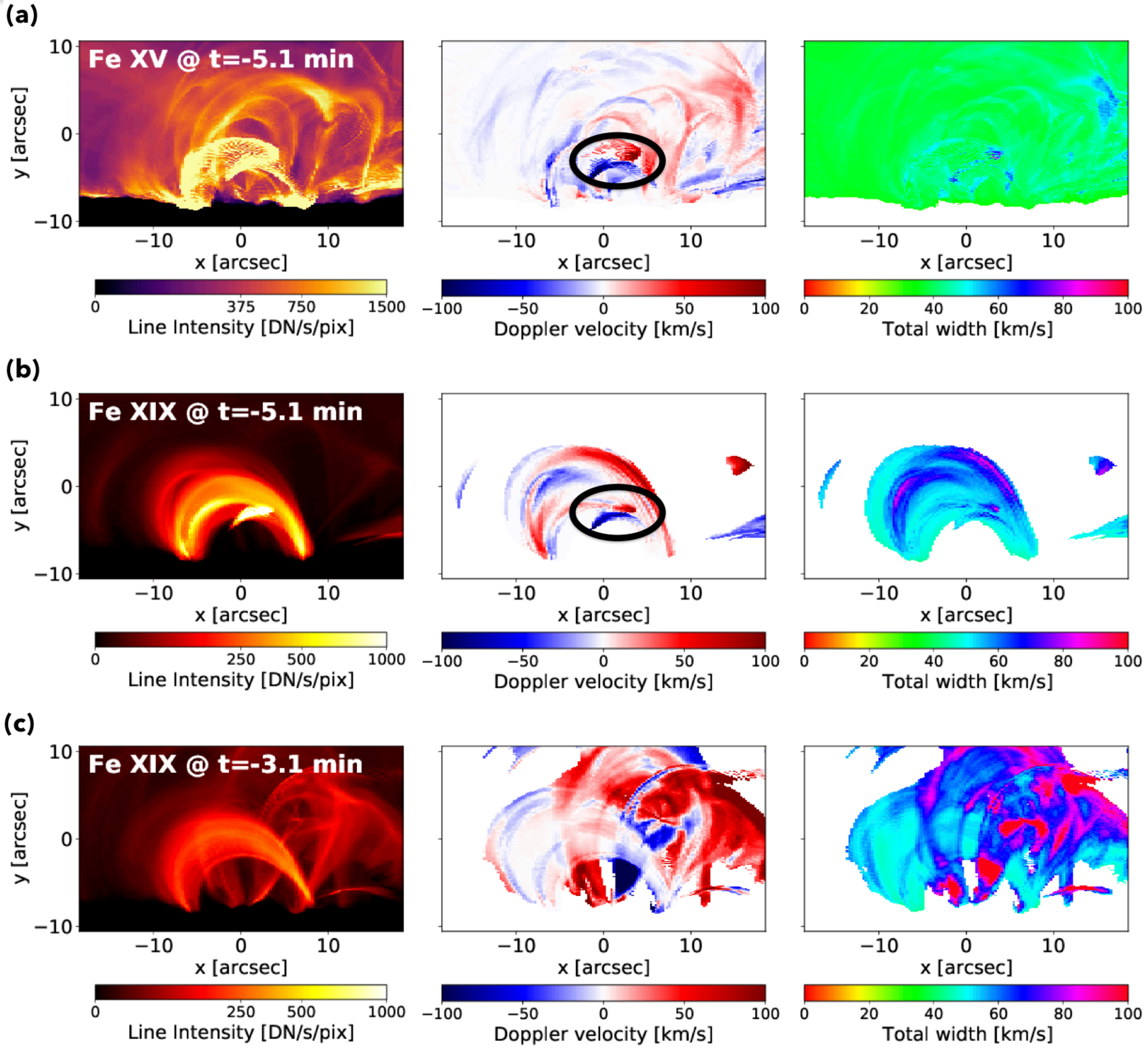

MUSE will provide spectroscopic signatures of triggers of flares and eruptions, which are often missed by single-slit instruments. Such observations will test existing models of solar eruptions which invoke different physical mechanisms. **Bidirectional flows show reconnection trigger.**

Cheung et al., 2022

MUSE will constrain initial plasma conditions of flux-rope-driven CME models

Fe XV (~ 2 MK) & Fe XXI (~10 MKL) moment maps of flare + nascent CME

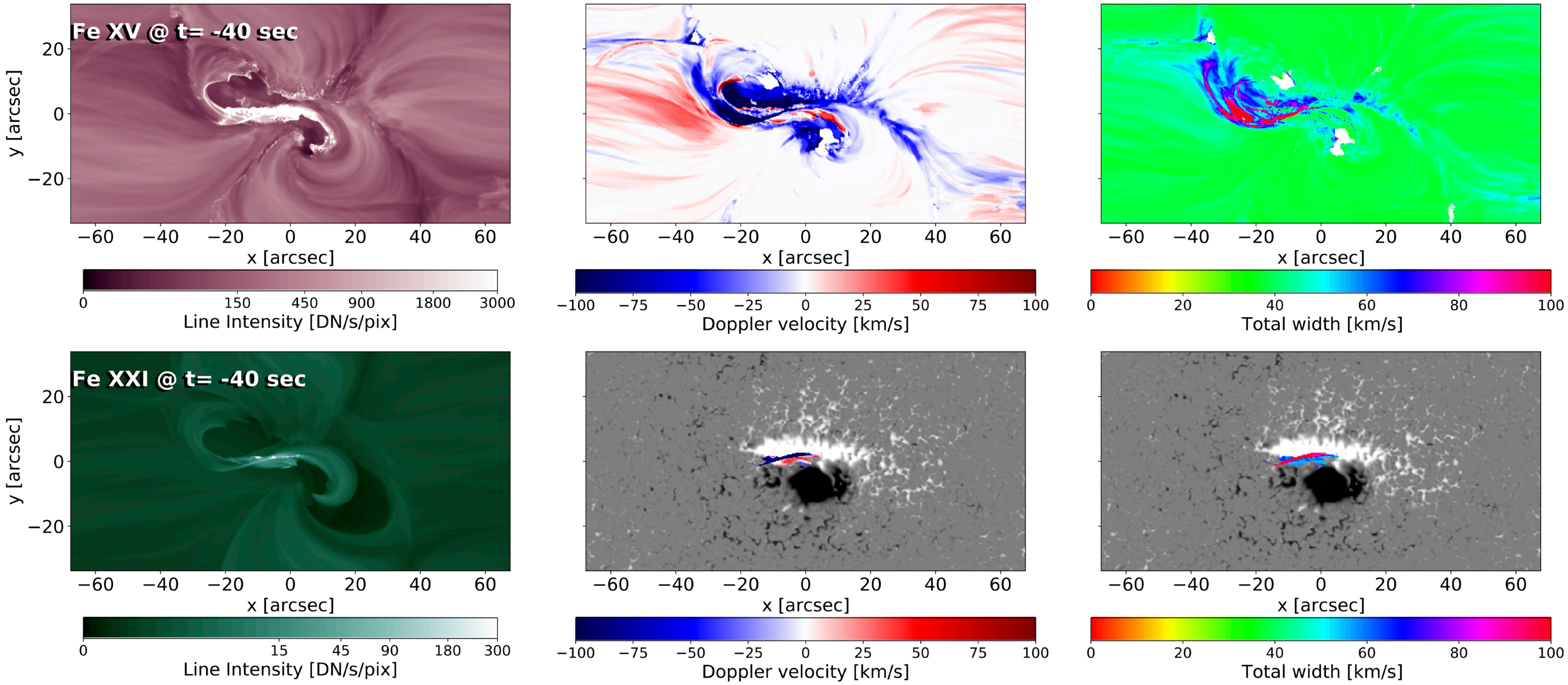

MUSE will constrain initial plasma conditions of flux-rope-driven CME models

Fe XV (~ 2 MK) & Fe XXI (~10 MKL) moment maps of flare + nascent CME

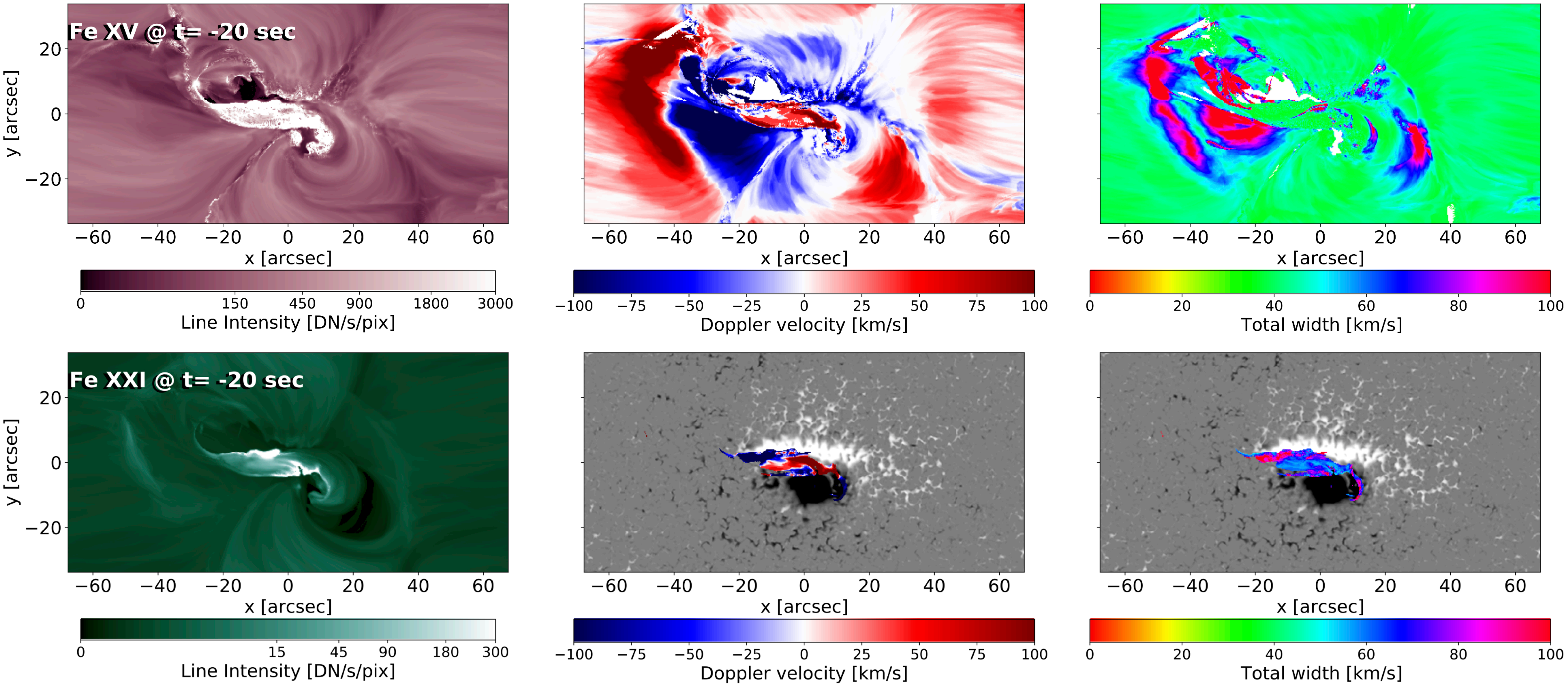

MUSE will constrain initial plasma conditions of flux-rope-driven CME models

- **Intensity, Doppler & line width maps of the source regions of CMEs constrain initial conditions of models (e.g. Jin et al. 2017 EEGGL module@ NASA CCMC can have new constraints).**

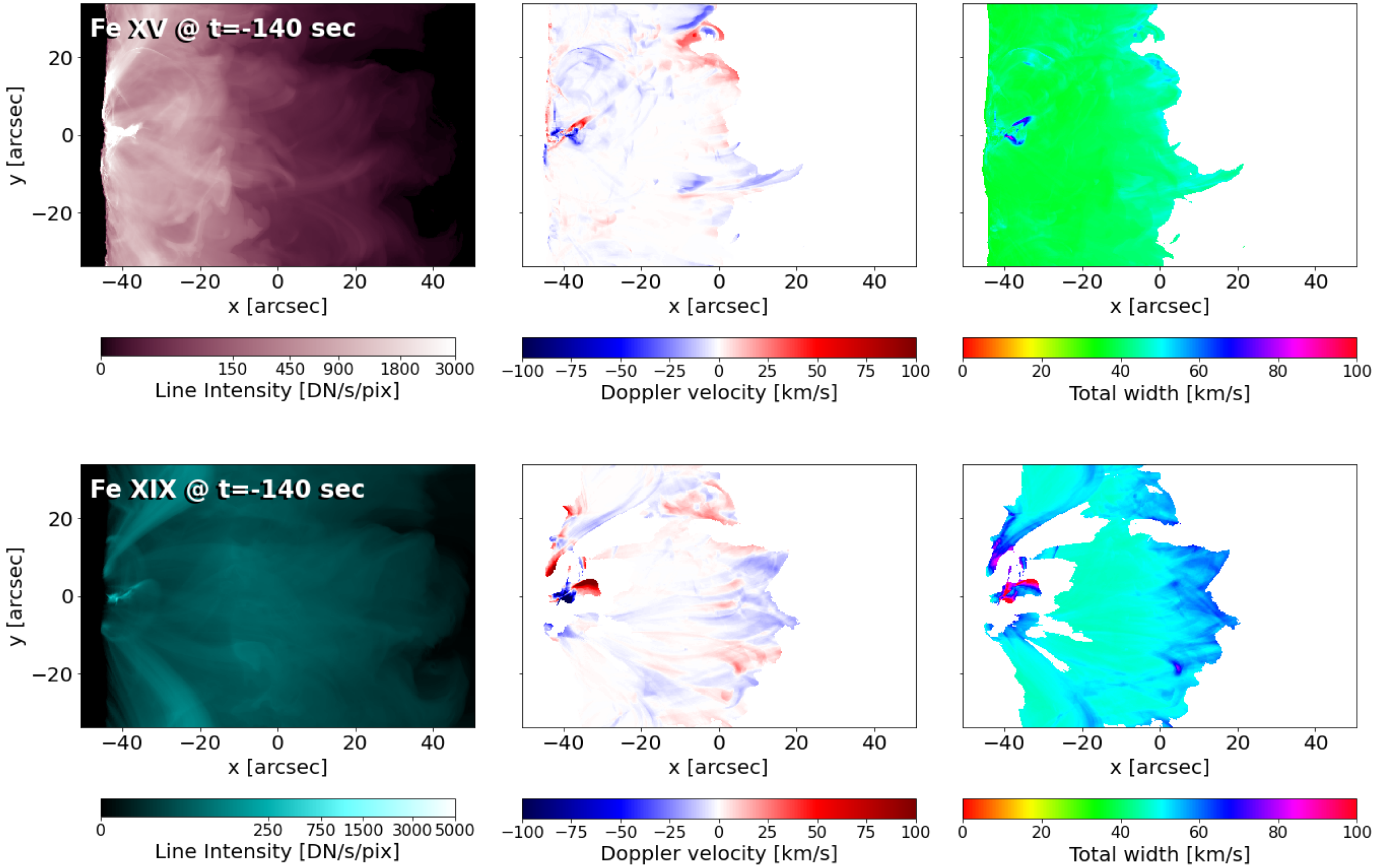

MUSE will provide constraints on models of the plasmoid instability

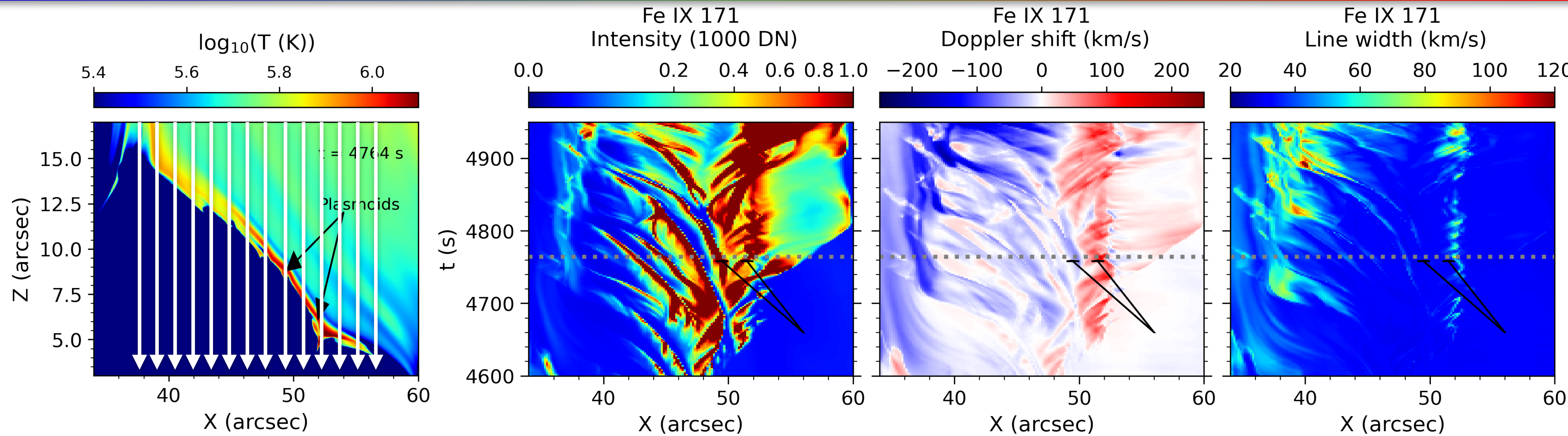

De Pontieu et al., 2022; Cheung et al., 2022

High-cadence, high resolution imaging spectroscopy by MUSE will capture the evolution of plasmoids at multiple scales (if and when they exist), testing the prediction of fast reconnection models mediated by the plasmoid instability.

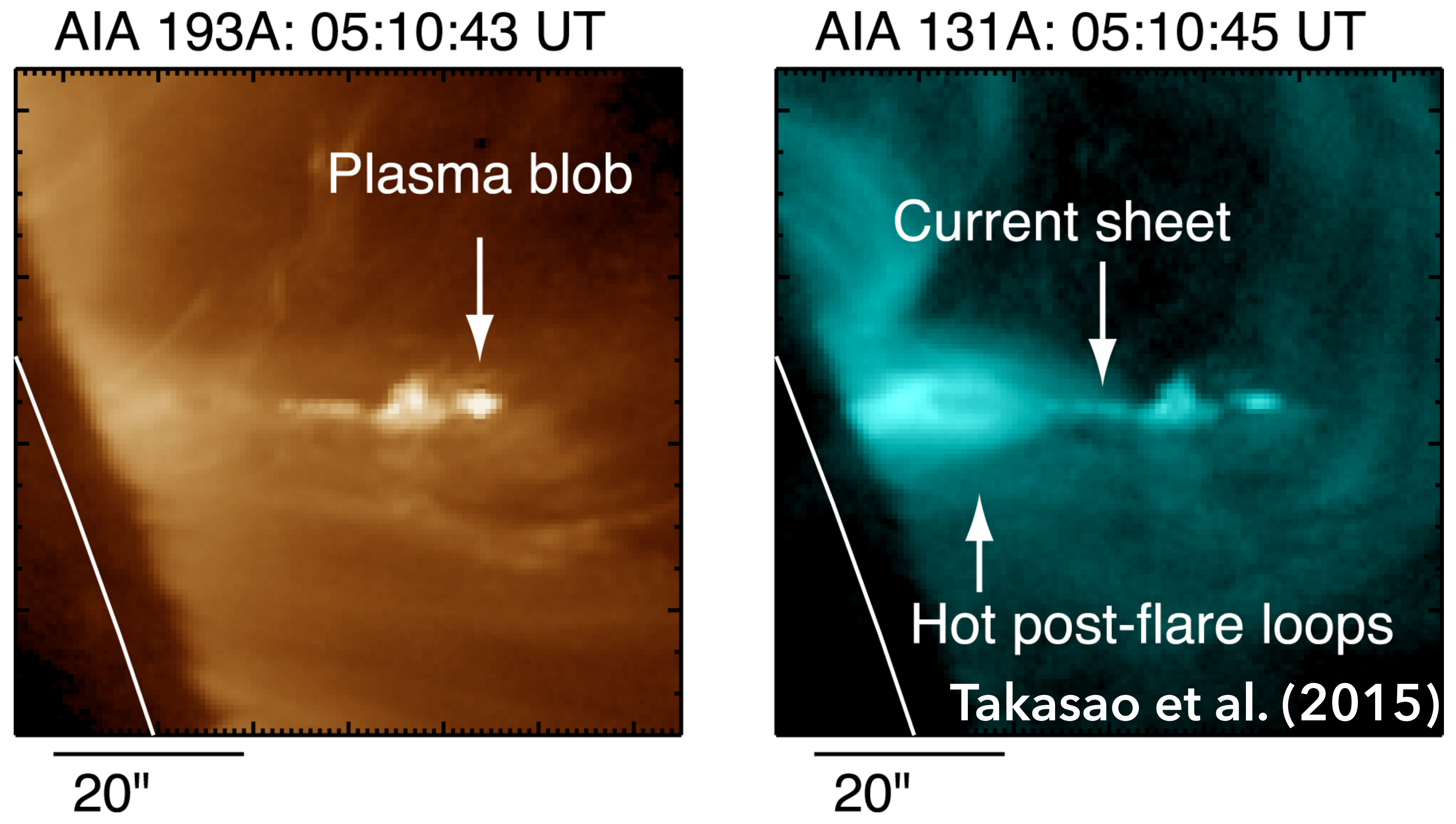

MUSE will test models of fast magnetic reconnection & particle acceleration

Models of reconnection outflows in flare current sheets (Takasao et al. 2015; Kong et al. 2019) predict multiple interacting fast mode shocks, which are candidate sites for particle acceleration.

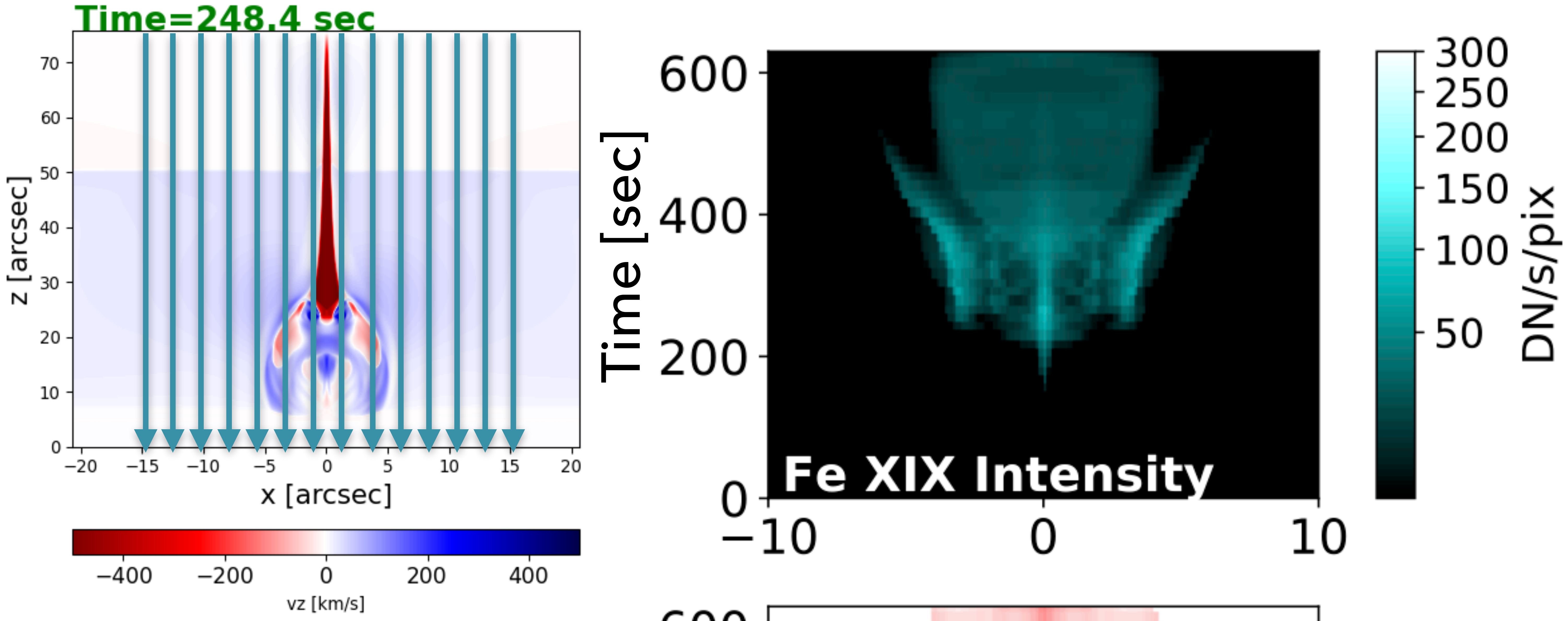

Cheung et al., 2022

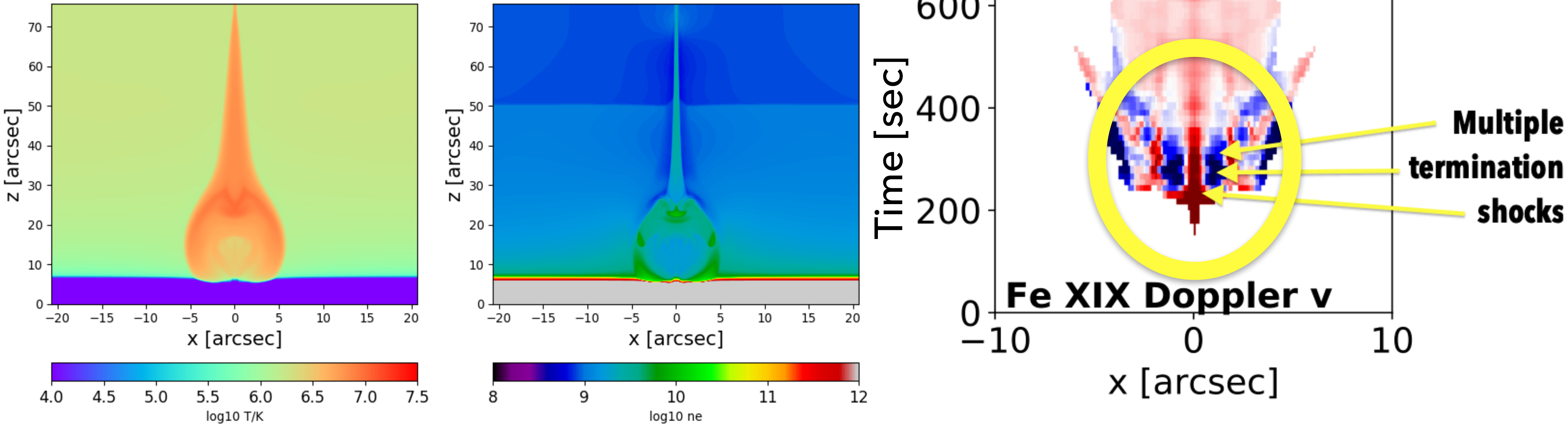

Open flux emanating from the edges of active regions is a source of the nascent solar wind. MUSE rasters will track how these regions evolves, and investigate the presence of waves and intermittency.

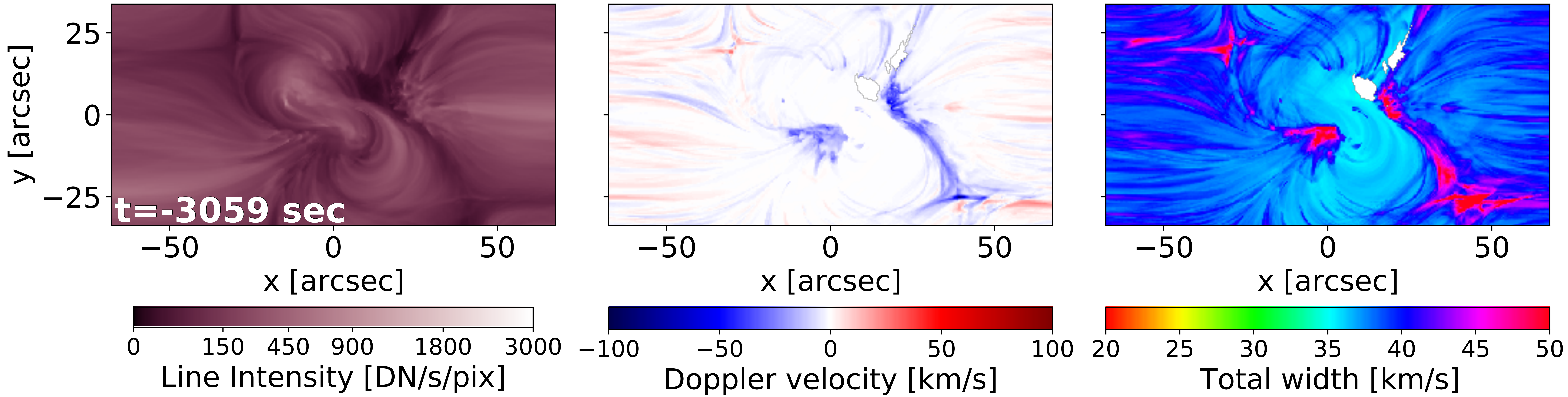

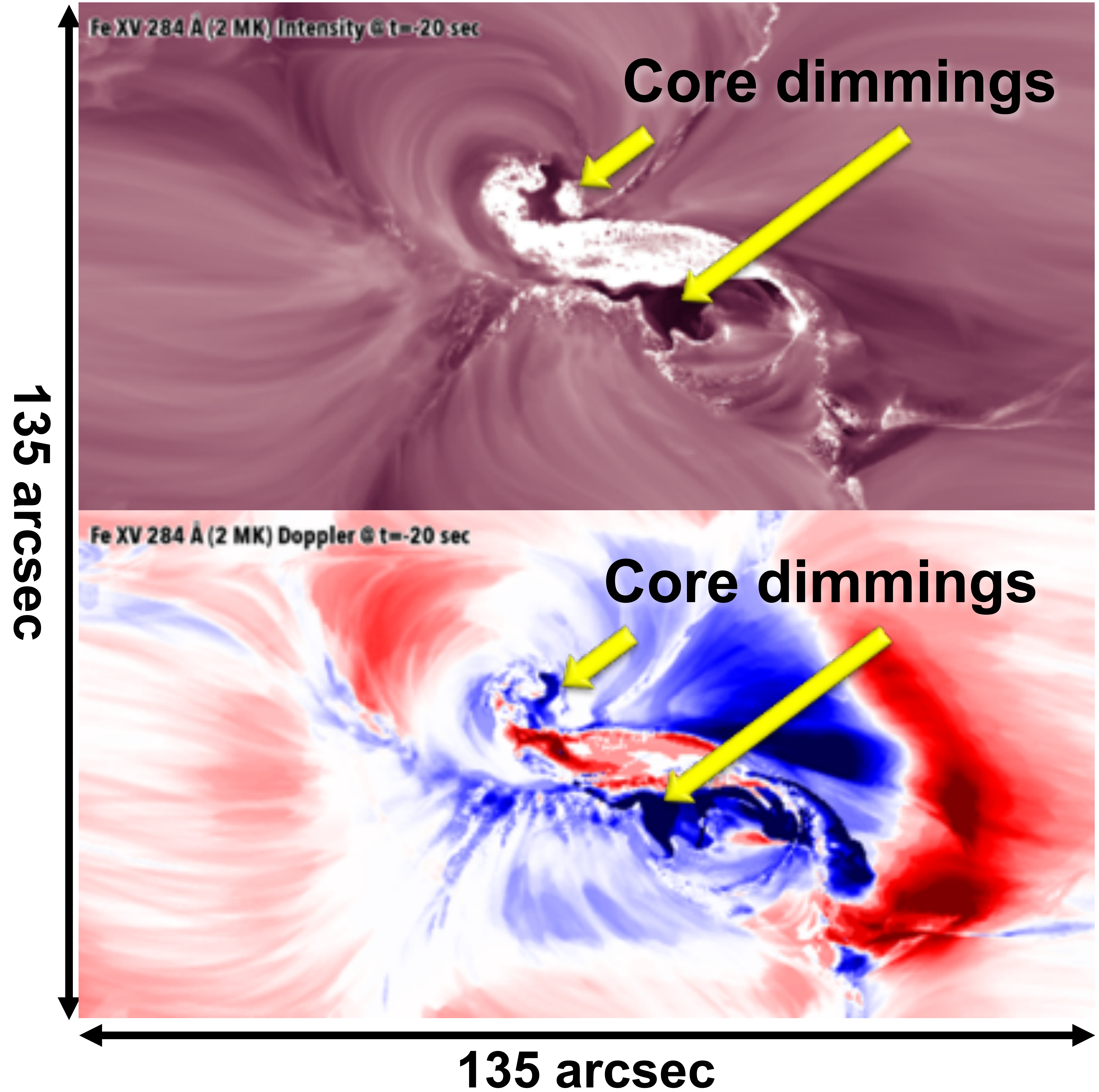

•High cadence MUSE multisite rasters (FOV covering up to 170”x170”) will reveal plasma properties in the core dimming regions, which are believed to be the footpoints of eruptive flux ropes.

Left: Fe XV (284 Å) intensity and Doppler velocity maps of simulated eruptive flare showing blueshifted flows in the core dimming region. (simulation from Cheung et al. 2022; Rempel, Chintzoglou & Cheung, 2023)

Discussion

What is the state of the art of 3D MHD simulations of flares and eruptions, and how do synthetic observables compare with observations?

- Increasingly realistic single-fluid MHD simulations reproducing the lifecycle of solar flares / eruptions.
- Models parameterizing fast electron heating produces hard x-ray sources at flare loop tops and footpoints (Ruan, Xia & Keppens 2020). The cause of the EM enhancement is still predominantly due to thermal conduction.
- Are non-thermal electrons energetically important for the energy budget of solar flares?
- Poor knowledge of 3D structure of the coronal field (Pariat's talk).

Which physical mechanisms are missing and which modelling advances are needed, also given the future availability of high-resolution observations from MUSE and other missions?

- Self-consistent particle acceleration in 3D flare models
- NLTE ion populations (c.f. Imada's talk) in 3D models - EUVST
- Loop evolution in 1D models with NLTE physics
- Multi-strand structuring & turbulence (other than Emslie & Bian 2018) - MUSE